

Simulation and optimization of pulsed RF irradiation scheme for chemical exchange saturation transfer (CEST) MRI – demonstration of pH-weighted pulsed-CEST MRI in acute ischemic stroke animal model

P. Z. Sun¹, E. Wang¹, J. S. Cheung¹, T. Benner¹, and A. G. Sorensen¹

¹Radiology, Athinoula A. Martinos Center for Biomedical Imaging, MGH and Harvard Medical School, Charlestown, MA, United States

Introduction Chemical exchange saturation transfer (CEST) imaging is an emerging MRI technique capable of imaging microenvironment properties including pH and temperature, and remains promising for clinical translation¹⁻⁴. However, CEST MRI contrast is complex. In addition to labile proton concentration and exchange rate, CEST contrast also depends on experimental parameters, particularly, RF irradiation power and scheme^{5,6}. Moreover, continuous wave (CW) RF irradiation is not available on most clinical systems due to hardware design limitation, for which, the pulsed RF irradiation scheme must be applied instead. Therefore, it is important to simulate and understand pulsed CEST MRI to help guide clinical translation.

Materials and Methods We simulated pulsed-CEST MRI in Matlab using representative relaxation parameters. The labile proton concentration relative to bulk water was assumed to be 1:500. We assumed a typical magnetic field strength of 4.7T, a total time of saturation (TS) of 3 s and a representative RF duty cycle of 50%. 1) Irradiation RF flip angle (ϕ) was varied from 45° to 540° with intervals of 45°, assuming a commonly used Gaussian shaped pulse and representative pulse duration of 15 ms. The exchange rate was varied from 10 to 100 s⁻¹ with intervals of 10 s⁻¹, while chemical shift ranged from 1 to 5 ppm per 0.25 ppm. 2) Irradiation RF pulse duration (τ). The RF flip angle was assumed to be 180°, and the RF pulse duration was increased stepwise from 5 to 30 ms, with an interval of 1 ms. 3) Comparison of pulsed- and CW-CEST MRI (both flip angle and pulse duration). CW- and pulsed-CEST MRI were simulated with the exchange rate varied from 10 to 100 s⁻¹, at intervals of 10 s⁻¹, for three representative chemical shifts of 1.9, 3.5 and 5 ppm. For each exchange rate and chemical shift, we used 2-dimensional variants of the RF flip angle and pulse duration: 150° to 270° with intervals 10°, and 1 to 5 ppm with intervals of 0.25 ppm, respectively.

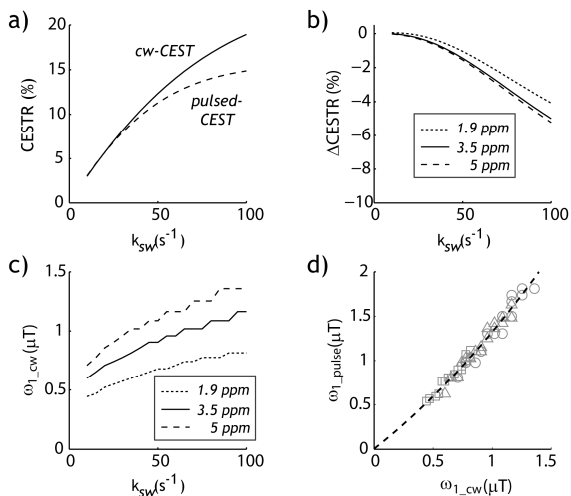


Fig. 1, pulsed CEST MRI dependence of exchange rate. a) Comparison of pulsed- and CW-CEST MRI. b) Pulsed-CEST is inefficient for imaging protons of high exchange rate. c) Optimal RF power for CW-CEST MRI d) Comparison of optimal pulsed-CEST with CW-CEST MRI.

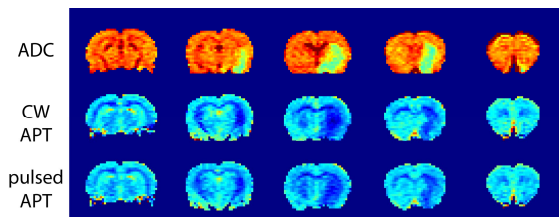


Fig. 2, in vivo evaluation of pulsed-APT MRI showed similar contrast as the conventional CW-APT MRI.

pulsed-CEST MRI to detect chemical exchange of relatively fast exchange rate⁷.

Acute ischemic stroke animals were imaged about 2 hrs after MCAO at 4.7T, as approved by SRAC. Animal's heart rate and blood pO₂ were continuously monitored online, and body temperature was maintained at the normal physiological range throughout the study. We used single shot echo planner image (EPI) as image readout. We used a FOV of 25x25 mm², with an image matrix of 64x64 and TR/TE=6000/28ms. Multi-parametric MRI of perfusion (ASL), diffusion (b=250 and 1000 mm²/s), CW-APT ($B_1=0.75$ uT, TS1/TS2=4.5s/0.5s) and pulsed-APT MRI ($\phi=\pi$, $\tau=15$ ms) were also acquired.

Results and Discussion We compared the pulsed-CEST contrast with the more commonly used CW-CEST MRI. Fig. 1a shows that for a representative chemical exchange rate range from 10 to 100 s⁻¹, the CW-CEST contrast is approximately equal to or higher than the pulsed-CEST contrast. We plotted the difference between pulsed-CEST and CW-CEST contrast as a function of exchange rate, which showed that the pulsed-CEST MRI became less effective than CW-CEST MRI contrast particularly at higher exchange rate, noticeably above 50 s⁻¹. In addition, the loss of pulsed-CEST contrast is greater at higher chemical shift, due to more efficient CW-CEST MRI (Fig. 1b). Fig. 1c shows the optimal RF amplitude for the CW-CEST MRI increases with exchange rate. In comparison, Fig. 1d shows the equivalent RF amplitude of pulsed-CEST MRI ($\bar{B}_1 = \phi/(\gamma\tau)$, where γ is the gyromagnetic ratio) with that of CW-CEST MRI (Fig. 1c). Importantly, the optimal RF amplitude for pulsed-CEST MRI can be reasonably estimated from B_1 field for CW-CEST MRI, being $B_{1_pulse}=0.28B_{1_cw}^2+1.038^*B_{1_cw}$. As such, our finding suggests that pulsed-CEST MRI experiments can be optimized based on the better-understood CW-CEST MRI, therefore, facilitating its in vivo applications.

The optimized pulsed-APT MRI was preliminarily evaluated in vivo using acute ischemic stroke animals. The ischemic lesion appeared as hypointensity in both ADC and pH-weighted APT maps (Fig. 2). Noteworthily, optimized pulsed-APT MRI showed similar contrast as commonly used CW-APT MRI. In summary, our study suggested that optimized pH-weighted CEST MRI is suitable to image endogenous amide proton CEST MRI, feasible for in vivo application and clinical translation. While on the other hand, alternative irradiation schemes have to be developed/optimized in order to apply

References 1)Ward et al. JMR 2000;143:79-87. 2)Zhou et al. Nat Med, 2003;9(8):1085-90. 3)Jokivarsi et al, MRM 2007;57(4):647-53. 4)Sun et al. 2007; 27(6):1129-36. 5)Woessner et al. MRM 2005;53:790-9. 6)Sun, JMR 2010;205(2):235-41. 7)Vinogradov et al, JMR 2005;176(1):54-63.